Mode-selective multiphoton excitation in a model system

Robert E. Wyatt*
Institute for Molecular Science, Okazaki 444, Japan

Gabriel Hose† and Howard S. Taylor†
Fundamenteel Onderzoek der Materie—Instituut voor Atoom- en Molecuulfysica (FOM Institute for Atomic and Molecular Physics), Kruislaan 407, 1098-SJ Amsterdam, The Netherlands

(Received 10 January 1983)

A computational study is made of mode-selective multiphoton excitation in a model nonseparable anharmonic-oscillator system. The time evolution of quantal wave packets on the Hénon-Heiles potential surface is treated via Floquet theory; periodicity of the classical laser field, $E_0\cos\omega t$, is utilized to formulate the propagator for the state amplitudes. In a previous study by Hose and Taylor, a criterion was developed by which the quantum states corresponding to the classical quasiperiodic motion are identified. Two types of quasiperiodic states exist in the Hénon-Heiles system: Q^{I}, the normal mode and Q^{II}, a local (bond) mode; highly mode-mixed states are designated as N (nonquasiperiodic). In the present study it is found that efficient multiphoton excitation into a subset of the Q^{I} states lying between the classical critical energy and the dissociation barrier is obtained, provided that the field strength is not too large and the frequency of the laser is tuned to the fundamental of the Q^{I} ladder. Implications for mode-selective excitation in real systems are discussed.

I. INTRODUCTION

With the advent of the availability of high-power lasers, the concept of photoselective multiphoton excitation and dissociation of molecules was advanced.[1–6] In photoselective excitation (PSE), it was envisioned that the monochromatic laser would excite the molecule through a special ladder of nuclear motion states into the dissociation region. This special ladder would be a subset of all states, roughly equally spaced in energy, and would have the property of being either a local- (bond-) mode sequence or a normal-mode sequence. Upon reaching the dissociative continuum, the molecule would fragment in a pattern that was a natural extension of the local or normal modes, respectively. This attractive idea immediately ran into difficulty as it was realized that it would be made unlikely by two dynamical effects. The first was anharmonicities which would detune the ladder spacings from the laser frequency. Power broadening could not generally be counted on to spread the rungs of the ladder to the correct energy. The second effect was the quantum-mechanical mixing of modes that would occur as the dissociation region was approached. Here the high density of local, normal, and other states would mix strongly. The states would lose their character and form a mode-mixed quasicontinuum. On one hand, the latter effect would promote multiphoton dissociation by insuring that an optically active state was available at most energies. On the other hand, it would cause the rung to be non-mode-specific and destroy the desired effect. Although some degree of mode selectivity is claimed in some early experiments,[7–10] most experiments and theory[11–12] seem to support the unavoidable occurrence of a mode-mixed quasicontinuum and hence nonspecific excitation and dissociation.

One of the first glimmers of hope that mode-mode mixing might be avoided came from classical mechanics. Computations on systems of two coupled anharmonic oscillators were expected to show that for all allowed initial conditions the resulting trajectory would eventually cover the available energy surface in phase space and the classical X-Y plane bounded by the potential walls. Amazingly, for certain initial conditions a finite number of classes of trajectories were found that seemed to be restricted to toroidal subshells of the phase-space energy surface and to specific regions of the allowed position space. These restricted trajectories were mostly nonperiodic, but were quasiperiodic (Q). Several recent reviews describe these results in more detail.[13–18] The fact is that restricted motion could occur in nonseparable systems and for reasons which were not immediately obvious. Moreover, action variables could be computed for quasiperiodic trajectories, giving rise *after the fact* to mathematical, but not physically evident, constants of the motion.

Two questions were obvious from these results. The first speculated that a quantum analog of the Q trajectories might reveal subsets of states, nested among the total set, that were nonmixing in the mode-mode sense, local or normal, and therefore usable as rungs on a selective photodissociation ladder. The second question asked what caused these quasiperiodic motions. In a recent paper by Hose and Taylor[19] both questions were addressed and answered. For a quantum two-dimensional anharmonic oscillator it was shown that Q states do exist as subsets of all states and that they have the following properties.

(i) The Q states are identified by purely quantum-mechanical methods, given the wave function $\Psi(x,y)$.

(ii) Q states have wave functions that are dominated by projections onto wave functions of systems that have rigorous constants of the motion. Hence, with high probability the Q states act as if they have extra "quasi" constants of the motion, i.e., they do not significantly mode-mix.

(iii) The Q levels were the only levels that could be ap-

TABLE I. Selective-excitation ladders in the Hénon-Heiles system; rungs in the Q^{I} (harmonic) ladder are characterized by large overlaps with TDHO states of the type $(n,\pm n)$; rungs in the Q^{II} ladder have significant overlap with states describing excitation along the cubic X mode, i.e., $(n_x^c\neq 0, n_y^h=0)$ (cf. Tables I–III in Ref. 19).

Q^{I} ladder					Q^{II} ladder				
Level	States	n	ϵ_n	$\epsilon_{n+1}-\epsilon_n$	Level	States	n_x^c	$\epsilon_{n_x^c}$	$\epsilon_{n_x^c+1}-\epsilon_{n_x^c}$
$37E$	111,112	13	14.085[a]		$34E$	102	14	13.584[a]	
$20A_1$	94	12	13.077	1.008	$19A_1$	90	13	12.774	0.810
$27E$	80,81	11	12.065	1.012	$17A_1$	77	12	11.970	0.804
$22E$	65,66	10	11.050	1.015	$23E$	67	11	11.152	0.818
$12A_1,7A_2$	54,55[b]	9	10.035	1.015	$19E$	57	10	10.318	0.834
$15E$	44,45	8	9.022	1.013	$16E$	46	9	9.444	0.874
$12E$	35,36	7	8.009	1.013	$13E$	38	8	8.576	0.868
$7A_1,3A_2$	27,28[b]	6	6.999	1.010	$10E$	29	7	7.659	0.894
$7E$	20,21	5	5.991	1.008	$8E$	23	6	6.765	0.948
$5E$	14,15	4	4.986	1.005	$6E$	16	5	5.817	0.948
$3A_1,1A_2$	9,10[b]	3	3.985	1.001	$4E$	12	4	4.899	0.918
$2E$	5,6	2	2.985	1.000	$3E$	7	3	3.926	0.973
$1E$	2,3	1	1.990	0.995	$2E$	5	2	2.985	0.941
$1A_1$	1	0	0.999	0.991	$1E$	2	1	1.990	0.995
					$1A_1$	1	0	0.999	0.991

[a]Rungs above the classical dissociation barrier, $D=13.333$.
[b]Nearly degenerate levels.

proximated by the Einstein-Brillouin-Keller (EBK) methods of semiclassical quantization.[20–23]

(iv) The Q states are also known[24] to be localized ($|\Psi(x,y)|^2$) in the same regions in the X-Y plane that are occupied by the Q trajectories that are used to obtain the corresponding Q levels by semiclassical EBK quantization.

For the Hénon-Heiles potential[23,25] it was shown[19] that two types of Q ladders exist (cf. Table I). *The Q^{II} ladder* comprises states whose wave functions are dominated by separable functions with the excitation primarily in the anharmonic X mode. The Q^{II} ladder is not amenable to PSE because it rapidly detunes due to its large anharmonicity. The other type of ladder, *called Q^{I}*, comprises states whose wave functions are dominated each by a subset of degenerate eigenstates of the two-dimensional harmonic oscillator (TDHO). The Q^{I} states are of a normal-mode type and are not mode-mode mixing as if they do not "feel" the anharmonicity in the potential. All the Q^{I} rungs (cf. Table I) correspond to TDHO states of the type $(n,\pm n)$ which for a given radial quantum number n have reached the highest possible absolute angular momentum quantum number, $|l|=n$. Note that the cubic anharmonicity of the potential couples TDHO states with $|l|>n-3$ to less states than it does the states with $|l|<n-3$. This is the physical reason why these Q^{I} states remain non-mode-mixed. Similar arguments hold for the high Q^{II} states. Qualitatively, both Q^{I} and Q^{II} ladder states represent extreme motion of the respective mode.

Hose and Taylor[19] quickly realized that the Q^{I} ladder, since it acted like a TDHO and would not detune or mode-mode mix, is perfect for selective multiphoton excitation provided the laser frequency would nearly fit its fundamental and the field intensities are not so high as to further mix (or detune) the states. The selection rules of the TDHO perfectly fit the Q^{I} ladder: $(n,\pm n)\leftrightarrow(n+1,\pm(n+1))$, that is, $|\Delta n|=|\Delta l|=1$. The high overlap between Q^{I} states and TDHO states indeed ensures high oscillator strengths. Not having the experience and programs to carry out multiphoton dynamics calculations, Hose and Taylor simply pointed out[19] that if one started in the ground state, which is essentially the TDHO ground state (0,0), and mentally defined a sequence of excitations chosen so as to minimize detuning and maximize the X- or Y-dipole matrix elements, that one could use the Q^{I} (and the system) fundamental to climb up the Q^{I} ladder. The last step in this ladder carries the system from the highest Q^{I} bound state to a continuum resonance state whose prime projection is of the Q^{I} type and is simply the next Q^{I} rung which missed being bound. From this resonance the system could dissociate or, in turn, climb higher to other resonant Q^{I} rungs from which it would eventually decay in what would be mode-specific or non-mode-specific dissociation. The Hose-Taylor discrete basis set calculation found Q resonances that were correlated with Q trajectories appearing above the classical dissociation barrier.[26,27] In a later calculation these Q roots were found to be stabilized. Coincidently, the Hose-Taylor criterion for finding quasiperiodic states, when satisfied for a continuum energy eigenfunction, turns out to be similar to the Taylor stabilization criterion.[28]

The key point is that, albeit a model system which is not a molecule but which exhibits features analogous to coupled bond anharmonicity and mode-mode mixing, one could anticipate, but not demonstrate, PSE and dissociation. The problem remained of obtaining a method that could do multiphoton excitation calculations for a given anharmonic-oscillator potential, namely, the Hénon-Heiles system. Recently, such a method has been developed and tested by Wyatt *et al.*,[29] who adopted Floquet theory for the computation of the time development operator in systems with large number of states. Interestingly, Davis *et al.*,[30] while carrying out calculations on the Hänsel system[31] of coupled Morse and harmonic oscillators, found a

behavior similar to what Hose and Taylor had predicted in the Hénon-Heiles system.[19] At a certain frequency, the harmonic-oscillator fundamental, the system seemed to climb a ladder of equally spaced states without energy spreading. The calculations at field frequencies differing from the harmonic fundamental showed excitation bottlenecks followed by energy spreading among many mode-mixed states. However, the Hose-Taylor-type analysis has not yet been done on the Hänsel system. The calculations of the present collaborative study demonstrate that PSE indeed occurs via a Q^{I} ladder, as anticipated, in the Hénon-Heiles system which is known to exhibit regions of severe mode-mode mixing.

II. THEORY

A. Quantum quasiperiodic states

In this subsection the Hose-Taylor criterion for the detection of quantum quasiperiodic states is reviewed.[19] Consider the Hénon-Heiles system of coupled anharmonic oscillators which is known to exhibit classical quasiperiodic and chaotic motion. The quantum Hénon-Heiles Hamiltonian is (dimensionless coordinates, $\hbar\omega=1$)

$$H=-\tfrac{1}{2}\left[\frac{\partial^2}{\partial x^2}+\frac{\partial^2}{\partial y^2}\right]+\tfrac{1}{2}(x^2+y^2)+\lambda\left[xy^2-\frac{x^3}{3}\right]$$
$$=-\tfrac{1}{2}\left[\frac{\partial^2}{\partial r^2}+\frac{1}{r}\frac{\partial}{\partial r}+\frac{1}{r^2}\frac{\partial^2}{\partial\theta^2}\right]+\tfrac{1}{2}r^2-\frac{\lambda r^3}{3}\cos 3\theta\ , \tag{2.1}$$

where $\lambda=0.1118$.[23] Note that the polar form of this Hamiltonian emphasizes the C_{3v} symmetry of the system; the quantum energy levels are therefore labeled as A_1, A_2, or E which are doubly degenerate.

Clearly, the Hamiltonian (2.1) is *not separable*. The first step in the analysis is to partition H into a separable part called H_s, and mode-mode coupling terms $H-H_s$. The only requirement from H_s is that it be a *simple* separable Hamiltonian. For a given nonseparable H many reasonable H_s's may be found. All of them should, in principle, be examined according to the procedure described below. However, in the application to the Hénon-Heiles system Hose and Taylor found that it is enough to consider the two most obvious H_s's which they denoted as H_s^{I} and H_s^{II}. The former Hamiltonian is of higher symmetry and the latter is of lower symmetry than the full Hénon-Heiles Hamiltonian.

H_s^{I} is the Hamiltonian of the TDHO,

$$H_s^{\mathrm{I}}=H+\frac{\lambda r^3}{3}\cos 3\theta\ , \tag{2.2}$$

where H is given by Eq. (2.1). The eigenstates of H_s^{I} are labeled by the radial quantum number n and the azimuthal number l. The states (n,l) are simultaneously eigenstates of H_s^{I} and the angular momentum L_θ. Each n labels thereof a degenerate subspace of states with l ranging from $-n$ to $+n$ in increments of two.

H_s^{II} is the Hamiltonian of two uncoupled oscillators, X mode (cubic) and Y mode (harmonic):

$$H_s^{\mathrm{II}}=H-\lambda xy^2=h_x^c+h_y^h \tag{2.3}$$

with the corresponding eigenstates labeled by the mode quantum numbers n_x^c and n_y^h. Aside from accidental degeneracy the spectrum of H_s^{II} is nondegenerate, and each pair of mode quantum numbers labels one energy subspace of H_s^{II}.

The second step in the analysis is to examine the expansion of the eigenstates of the full Hamiltonian in terms of the eigenfunctions of the separable Hamiltonians. The Hose-Taylor criterion says that an eigenstate of H is quasiperiodic with respect to a certain H_s (e.g., H_s^{I} or H_s^{II}) if the squared magnitude of the overlap of its wave function with any degenerate subspace of that H_s exceeds 0.5. Accordingly, the Hénon-Heiles states are labeled as Q^{I}, Q^{II}, or N, where the latter are nonquasiperiodic, meaning that the squared-magnitude overlap with any particular degenerate subspace of either H_s^{I} or H_s^{II} is always less than or equal to 50%.

When applied to the Hénon-Heiles system the Hose-Taylor criterion reproduced the known classical picture in this system.[25] At low energies all the quantum states are quasiperiodic (either Q^{I}, Q^{II}, or both); at high energies most of the states are nonquasiperiodic (N) and very few are Q^{I} or Q^{II}. A small transition region between these two behaviors begins just below the classical critical energy $E_c\approx 8.67$, where the Kolmogorov-Arnold-Moser (KAM) transition from highly quasiperiodic to highly chaotic motion occurs. Moreover, there is a remarkable agreement between the purely quantum results of Hose and Taylor[19] and the semiclassical results of Noid and Marcus,[23] who had identified several quasiperiodic levels in this system with the use of EBK quantization techniques.

The requirement for the 50% squared-magnitude overlap is needed to ensure that for the state in question there exists an energy-independent approximation to the effective Hamiltonian which is defined on the particular subspace of H_s.[32] This energy-independent effective Hamiltonian may be calculated to any desired accuracy by a convergent iteration method and will yield the exact energy of the eigenstate of the full Hamiltonian while operating on the part of the wave function that lies in the subspace. The degeneracy requirement from the subspace is to ensure that the effective Hamiltonian will commute with H_s, the separable Hamiltonian, which will thereby become a quasiconstant of the motion for that particular eigenstate of H. This means that the major part of the corresponding wave function (over 50%) is also an eigenfunction of H_s. Depending on the functional content of the degenerate subspace of H_s (singly degenerate, etc.) other quasiconstants of the motion may exist.[19] For example, in the Hénon-Heiles system, Eq. (2.1), it was found that all states that could be obtained by semiclassical EBK quanti-

TABLE II. Dipole functions $\mu(x,y)$.

Designation	Function
μ_1	x
μ_2	$0.9x+0.1x^2$
μ_3	y
μ_4	$0.45(x+y)+0.033(x^2+xy+y^2)$

zation of quasiperiodic trajectories[23] had to have two quasiconstants of the motion: either H_s^I and L_θ^2 or h_x^c and h_y^h. These states are of particular interest in the present context as they are essentially normal- or local-mode states which do not mode mix. Further discussion of these Q states and the description of the energy-level structure in this system will be given in Sec. III A.

B. Dipole functions

In the semiclassical dipole approximation the Hamiltonian describing a molecule interacting with a single-mode laser field $E_0\cos\omega t$ is

$$H'(t)=H-\mu\cos\phi(E_0\cos\omega t)\ , \tag{2.4}$$

where H is the Hamiltonian of the isolated molecule, for example, the Hénon-Heiles Hamiltonian Eq. (2.1); μ is the molecular dipole function and ϕ is the angle between the dipole moment and the direction of the applied field. To simplify the picture we assume $\cos\phi=1$ and concentrate solely on the effect of the laser parameters, i.e., E_0 and ω.

Assuming a dipole moment for the Hénon-Heiles system, we expand $\mu(x,y)$ about the origin and truncate the expansion at second order,

$$\mu(x,y)=\mu^0+\mu_x^0x+\mu_y^0y+\tfrac{1}{2}\mu_{xx}^0x^2+\mu_{xy}^0xy+\tfrac{1}{2}\mu_{yy}^0y^2\ . \tag{2.5}$$

Four dipole functions were constructed with the use of the above expression. The coefficients, shown in Table II, were chosen so that the largest matrix elements would have about the same magnitude in all four dipole matrices. In all cases μ^0 was set to zero as it cannot contribute to transitions between states. Dipole matrix elements $\mu_{ij}=\langle i\,|\,\mu\,|\,j\rangle$ were computed with the use of a 465-term expansion of Hénon-Heiles eigenstates in products of harmonic-oscillator functions in the X and Y coordinates.

C. Time evolution: Floquet theory

The response of a quantum state Ψ, associated with the molecular Hamiltonian H, to the classical single-mode laser field $E_0\cos\omega t$ will be treated with the use of Floquet theory. This theory takes advantage of the periodicity of the driving field in formulating the propagator which advances the state amplitudes forward in time. For completeness, a brief overview of the Leasure, Milfeld, and Wyatt[29] utilization of the Floquet method is presented below.

The time-dependent molecular wave function, when the field is turned on ($t>0$), is expanded in a finite set of *molecular eigenstates*

$$\Psi_i(x,y,t)=\sum_{j=1}^{N}C_{ji}(t)\psi_j(x,y)\ , \tag{2.6}$$

where i denotes the initial ($t=0$) stationary molecular state. The state amplitudes evolve in time by the $N\times N$ propagation matrix,

$$\underline{C}(t)=\underline{U}(t,0)\underline{C}(0) \tag{2.7}$$

with the initial condition $\underline{U}(0,0)=\underline{C}(0)=\underline{1}$. Inserting the time-dependent Hamiltonian (2.4) and the expansion of Ψ_i in molecular eigenstates into the Schrödinger equation yields the usual set of coupled first-order differential equations for the amplitudes $C_{ji}(t)$ or, in turn, the propagator elements $U_{ji}(t)$:

$$i\hbar\dot{U}_{ji}=\epsilon_iU_{ji}+\sum_{k=1}^{N}\mu_{jk}U_{ki}E_0\cos\omega t\ , \tag{2.8}$$

where ϵ_i is the stationary energy of the ith molecular state and the μ_{jk} are the dipole coupling elements.

At this point we shift emphasis from the "fundamental" amplitudes $\underline{C}(t)$ to Floquet amplitudes

$$\underline{F}(t)=\underline{\Phi}(t)e^{i\underline{\mu}\omega t},\quad \underline{\Phi}(t+\tau)=\underline{\Phi}(t) \tag{2.9}$$

which are products of functions periodic over the optical cycle ($\tau=2\pi/\omega$) and a periodic exponential term whose arguments are linear in t. $\underline{\mu}$, the characteristic exponent matrix, is a real-valued $N\times N$ diagonal matrix. Propagating $\underline{F}(t)$ across the first optical cycle $[0,\tau]$ with $\underline{U}(\tau,0)$, and rearranging the propagation equation $\underline{F}(t)=\underline{U}(\tau,0)\underline{F}(0)$, leads to the matrix eigenvalue equation

$$\underline{\Phi}^\dagger(0)\underline{U}(\tau,0)\underline{\Phi}(0)=e^{2i\pi\underline{\mu}}\ . \tag{2.10}$$

Solution of this equation gives the characteristic exponents μ_m (eigenvalues of $\underline{\mu}$), and the periodic functions $\underline{\Phi}$ at $t=0$. For any time which is a multiple of the optical period, $t=n\tau$, use of $\underline{F}(n\tau)=\underline{U}(n\tau,0)\underline{F}(0)$ immediately gives an explicit factored form for the propagator:

$$\underline{U}(n\tau,0)=\underline{\Phi}(0)e^{i\omega n\tau\underline{\mu}}\underline{\Phi}^\dagger(0)\ . \tag{2.11}$$

The fundamental (state-to-state) transition amplitudes are then given by $C_{ji}(n\tau)=U_{ji}(n\tau,0)$. The Floquet formalism may also be used to generate $\underline{U}$ at an arbitrary t which is not a multiple of τ.[29] However, this is not necessary in the present study.

In order to evaluate $\underline{\Phi}(0)$ and $\underline{\mu}$ from Eq. (2.10) the propagation matrix is needed at the end of the first optical cycle. Several routes are available to evaluate $\underline{U}(\tau,0)$ including direct numerical integration of the coupled equations (2.8), but in this study we have used the second-order Magnus approximation [cf. Eqs. (2.23)–(2.29) in Ref. 29(a)]. This approximation has been extensively tested for both single- and multiple-photon transitions.[29] One- and two-photon transitions are accurately handled, and approximations are provided for transitions of three, four, or more photons. For the purposes of the present study this level of approximation is sufficient.

In summary, Floquet theory provides a nonperturbative method for treating the response of a quantized system to a classical driving field. The advantage in this method is that all the numerical effort is concentrated in solving Eq. (2.10) at the end of the first optical cycle. Subsequent time evolution follows trivially via Eq. (2.11).

Once the fundamental amplitudes are obtained as a function of t, it is then straightforward to evaluate both instantaneous quantities and long-time averages. In the present context of multiphoton excitation we will be interested in properties involving the ground state ($i=1$). These are defined as follows:

(i) instantaneous transition probabilities from the ground state to the molecular state j,

$$P_j(t)=|\,C_{j1}(t)\,|^2\ ; \tag{2.12}$$

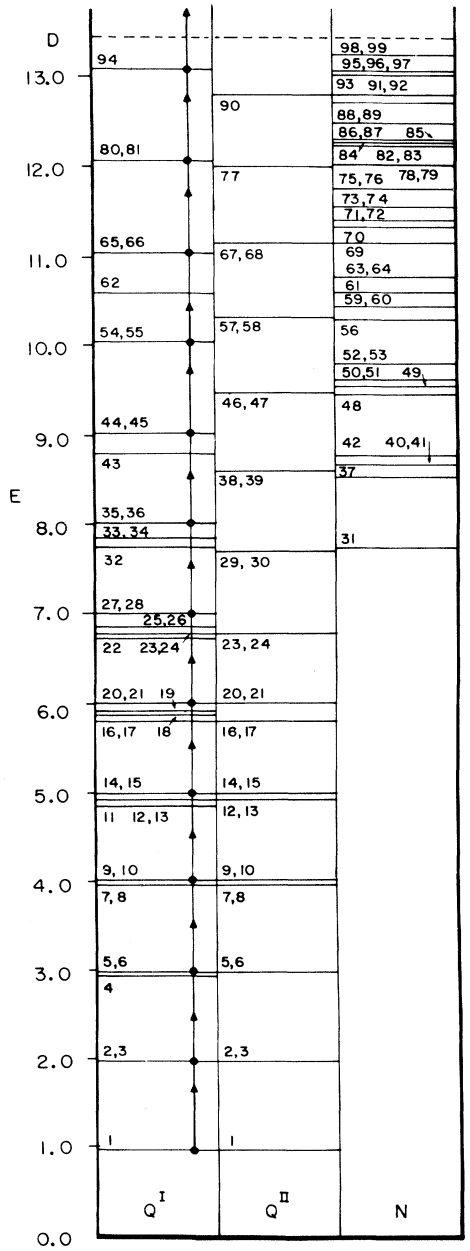

FIG. 1. Energy-level diagram for the Hénon-Heiles Hamiltonian, Eq. (2.1). Levels are grouped into columns according to their types, Q^{I}, Q^{II}, or N (cf. text for details). Energies are from Tables I–III of Ref. 19; the numbering of the states follows their order of appearance in these tables. Near degeneracies of A levels are unresolved in this diagram (e.g., states 9 and 10).

(ii) average number of photons absorbed from the ground state at time t,

$$n(t)=\sum_{j=2}^{N} P_j(t)(\epsilon_j-\epsilon_1)/\hbar\omega \ ; \tag{2.13}$$

(iii) long-time average transition probabilities,

TABLE III. Average magnitude of dipole coupling elements $\langle i\,|\,\mu\,|\,j\rangle$ for states in the Q^{I} ladder (cf. Table I) above E_c; coupling elements included in the average satisfy $0.9\hbar\omega \le |\epsilon_i-\epsilon_j| \le 1.1\hbar\omega$ with $\hbar\omega=1.0$; coupling elements of magnitude below 0.01 were excluded from the average.

Dipole function[a]	$Q^{\mathrm{I}}\cdots Q^{\mathrm{I}}$	$Q^{\mathrm{I}}\cdots Q^{\mathrm{II}}$	$Q^{\mathrm{I}}\cdots N$
μ_1	0.87	0.06	0.08
μ_2	0.77	0.06	0.34
μ_3	0.91	0.06	0.35
μ_4	0.71	0.03	0.23

[a]Cf. Table II.

$$P_j=\lim_{T\to\infty}\frac{1}{T}\int_0^T P_j(t)dt$$
$$=\sum_{n=1}^{N}|\phi_{1n}(0)|^2\,|\phi_{nj}(0)|^2, \tag{2.14}$$

where $\phi_{nj}(0)$ is the nth molecular component of the jth Floquet mode at $t=0$; and

(iv) long-time average number of photons absorbed,

$$\langle n\rangle=\sum_{j=2}^{N} P_j(\epsilon_j-\epsilon_1)/\hbar\omega \ . \tag{2.15}$$

All these quantities are evaluated for the Hénon-Heiles system with the use of the dipole functions in Table II.

III. MULTIPHOTON EXCITATION IN THE HÉNON-HEILES SYSTEM

A. Energy levels and multiphoton excitation ladders

The Hénon-Heiles Hamiltonian Eq. (2.1) has 99 quasibound states grouped into 66 energy levels below the classical dissociation energy, $D=13.333$. Of these states, 44 are of type Q^{I}, 22 are of type Q^{II} (15 states below E_c are both Q^{I} and Q^{II}), while 48 states are of type N (i.e., neither Q^{I} nor Q^{II}). Figure 1 is an energy-level diagram in which the Q^{I} levels are shown in the left column, the middle column shows the Q^{II} levels, and the right column the N-type levels. As the Hénon-Heiles Hamiltonian has C_{3v}

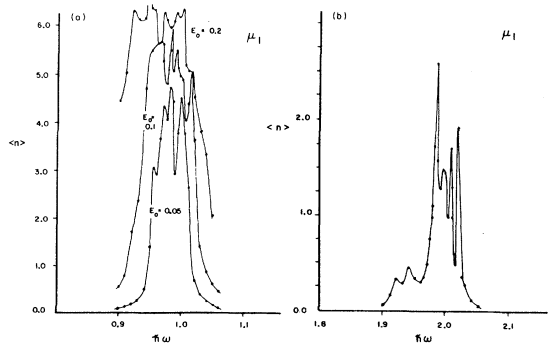

FIG. 2. Average number of photons absorbed from the ground state as function of frequency for the dipole function μ_1. (a) $E_0=0.05$, 0.10, and 0.20; (b) $E_0=0.5$.

symmetry, there are several degenerate E levels in the spectrum. In case of Q^{I} E levels both states are Q^{I}. This is frequently not the case with Q^{II} E levels, particularly above E_c where only one state of the degenerate pair is Q^{II} (cf. Tables I–III in Ref. 19). This is due to the fact that H_s^{II} has a lower symmetry than the total Hénon-Heiles Hamiltonian. Note that the density of N states increases rapidly above the critical energy. Roughly 60% of the states are above E_c and about 70% of them are N states as compared to about 10% below the critical energy.

A significant feature of the energy spectrum in this system, as was pointed out by Noid *et al.*,[33] is the existence of sequences of levels in which the energy separation between successive states is nearly constant. For example, in Table II a subset of the Q^{I} states forms a ladder in which the spacings between the rungs are constant with 2.4%. Multiphoton excitation up this ladder with photons of frequency $\hbar\omega \approx 1.0$ would require 13 photons for dissociation (cf. the left column in Fig. 1). Now, the states in this Q^{I} ladder are characterized by large overlaps with the TDHO wave functions $(n, \pm n)$, for which the azimuthal quantum number l has reached its highest allowed absolute value.[19] For comparison, the left column of Table II shows a subset of Q^{II} states which have large overlaps with the eigenstates of H_s^{II} that describe successive excitations in the cubic X mode and zero excitation in the harmonic Y mode.[19] The Q^{II} ladder is evidently very anharmonic and, although it reaches the dissociation region, it is clearly not a favorable route for multiphoton excitation as after the first few steps it detunes from the fundamental frequency.

Another important feature of the Q^{I} ladder which, as Hose and Taylor[19] point out, is quite general for quasiperiodic ladders of any kind is that due to the requirement of large overlap with the separable functions, the selection rules of the separable system apply to a good approximation to the Q ladders. Looking in Table II it is seen that the effective radial quantum number n and the magnitude of the azimuthal number $|l|$ increases by unity as one climbs from one Q^{I} rung to the next. This precisely fits the linear dipole selection rules for the TDHO, and it is therefore predicted on this basis that the Q^{I} ladder is indeed a serious candidate for PSE in this system. We would like to emphasize at this point that it is not a general phenomena that Q ladders obey favorable selection rules as does this Q^{I} ladder; in other systems even Q^{I}-type ladders may not do so.

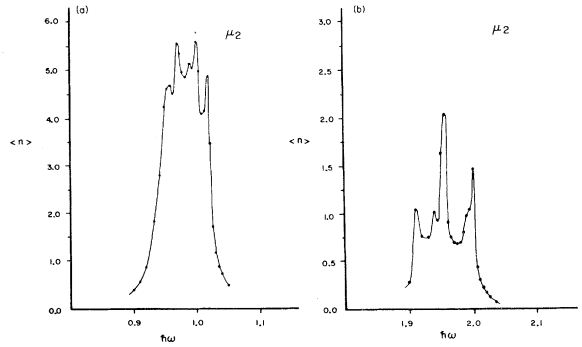

FIG. 3. Average number of photons absorbed from the ground state as function of frequency for the dipole function μ_2. (a) $E_0=0.1$; (b) $E_0=0.5$.

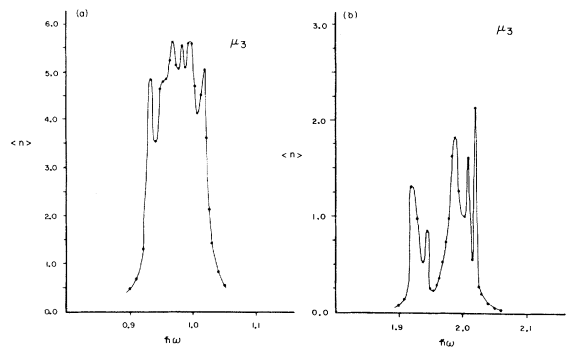

FIG. 4. Same as Fig. 3 but for dipole function μ_3.

In our discussion so far we have avoided the N states. However, we do not ignore them, but it so happens that in this system they only appear at high energies and therefore cannot participate in the first steps of the multiphoton absorption (cf. Fig. 1). Nevertheless, above E_c the N states are in the majority, and once the system reaches this region, the N states cannot be discarded from the excitation process. Table III shows the average magnitude of dipole couplings involving the Q^{I} ladder states above the critical energy. These averages include only the couplings between states separated by $\hbar\omega = 1.0 \pm 0.1$, i.e., 10% off the fundamental. It is clear that for all four dipole functions employed in this study, the $Q^{\mathrm{I}} \cdots Q^{\mathrm{II}}$ couplings are negligible and the $Q^{\mathrm{I}} \cdots Q^{\mathrm{I}}$ are greater than the $Q^{\mathrm{I}} \cdots N$ couplings. Yet, the couplings of Q^{I} ladder states to N states above E_c is certainly not small. It is precisely the purpose of this paper to show that although Q^{I} ladder states couple to mode-mixed states, that under suitable laser conditions a high degree of PSE may be achieved. This will be demonstrated in the remainder of this section.

B. Average number of photons absorbed

In order to identify the laser conditions leading to maximum absorption, the variation of $\langle n \rangle$, Eq. (2.15), with the laser parameters E_0 and ω was studied for the four dipole functions listed in Table II. The absorption spectra

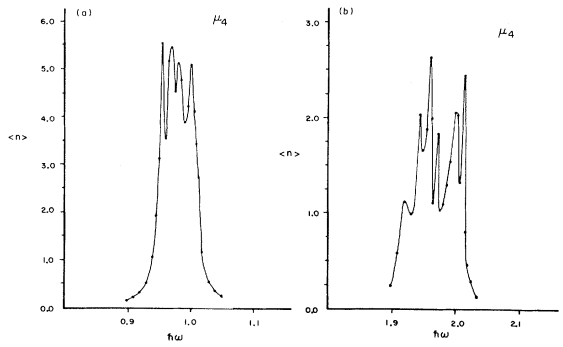

FIG. 5. Same as Fig. 3 but for dipole function μ_4.

TABLE IV. Long-time average probabilities (cf. text for details) as a function of laser parameters computed with the dipole function μ_1.

$\hbar\omega$	E_0	$\langle n \rangle$	P_b	$P_{\rm I}$	$P_{\rm II}$	P_N	P_c	$P_c^{\rm I}/P_c$
0.900	0.05	0.092	1.000	1.000	0.996	0.000	0.000	0.000
0.900	0.10[a]	0.507	0.998	0.991	0.957	0.004	0.007	0.007
0.900	0.20	4.400	0.953	0.767	0.731	0.137	0.183	0.062
0.950	0.05	1.368	0.990	0.928	0.884	0.054	0.046	0.166
0.950	0.10	5.450	0.978	0.601	0.536	0.297	0.293	0.045
0.950	0.20	6.280	0.959	0.607	0.514	0.271	0.328	0.117
0.965	0.10	5.631	0.959	0.707	0.497	0.226	0.233	0.211
0.975	0.10	4.785	0.965	0.792	0.597	0.168	0.193	0.285
0.982	0.10	5.937	0.944	0.734	0.523	0.187	0.272	0.156
0.985	0.10	5.026	0.967	0.863	0.541	0.119	0.115	0.406
0.990	0.10	5.462	0.966	0.862	0.461	0.130	0.270	0.534
1.000	0.05	4.472	0.999	0.990	0.594	0.009	0.259	0.960
1.000	0.10	4.899	0.995	0.917	0.574	0.055	0.271	0.700
1.000	0.20	6.307	0.948	0.715	0.457	0.229	0.344	0.310
1.005	0.10	4.016	0.996	0.996	0.625	0.004	0.184	0.980
1.015	0.10	5.036	0.999	0.932	0.552	0.036	0.326	0.791
1.980	0.50	0.291	0.999	0.994	0.982	0.002	0.001	0.135
1.987	0.50	2.601	0.997	0.997	0.562	0.003	0.337	0.990
1.995	0.50	1.283	0.999	0.998	0.762	0.002	0.129	0.984
1.997	0.50	1.463	0.999	0.997	0.772	0.002	0.164	0.982
2.005	0.50	0.990	0.999	0.997	0.850	0.003	0.105	0.973
2.010	0.50	1.710	0.999	0.979	0.687	0.020	0.144	0.853
2.017	0.50	0.464	0.999	0.999	0.944	0.001	0.032	0.967
2.020	0.50	1.926	0.989	0.938	0.634	0.060	0.293	0.790

[a]Assuming a molecular dipole of 1 debye, we have estimated from the power broadening and the fundamental level spacing that $E_0=0.1$ would roughly correspond to a laser power of 50 GW/cm^2.

shown below were all calculated with the use of a basis of 110 Hénon-Heiles eigenstates; the top 11 states provide a crude "discretization" of the continuum above the classical dissociation barrier, $D=13.333$. On the basis of calculations done with fewer numbers of states,[29] we expect these results to show the main qualitative features of the absorption spectra in the presence of the "true" continuum. The same basis was employed in the calculations reported in Secs. III C and III D. A total of 214 Floquet time-evolution calculations were performed for all four dipole functions, each requiring about three minutes of central-processing-unit (CPU) time on the Hitachi M-200H computer.

Figures 2—5 display $\langle n \rangle$ for the four dipole functions. The dots indicate the calculated values, the smooth curves were drawn between the dots for visual purposes only. Sharp peaks and valleys due to high-order multiphoton absorption may have been missed. Part (a) of each of these figures is the spectrum near $\hbar\omega=1.0$ for $E_0=0.1$ [except for Fig. 2(a)]; part (b) shows the overtone spectrum near $\hbar\omega=2.0$ for $E_0=0.5$.

Plots of $\langle n \rangle$ versus $\hbar\omega$ computed with the use of the dipole function μ_1 for three field strengths $E_0=0.05$, 0.10, and 0.20 are shown in Fig. 2(a). The sharp absorption peaks appearing between $\hbar\omega=0.9$ and 1.1 are due to high-order multiphoton absorptions. Note the decreased

TABLE V. Long-time average probabilities (cf. text for details) as a function of laser frequency computed with the dipole function μ_2; $E_0=0.1$ for $\hbar\omega\approx1.0$, $E_0=0.5$ for $\hbar\omega\approx2.0$.

$\hbar\omega$	$\langle n \rangle$	P_b	$P_{\rm I}$	$P_{\rm II}$	P_N	P_c	$P_c^{\rm I}/P_c$
0.990	5.033	0.982	0.881	0.503	0.114	0.255	0.558
1.005	4.073	0.999	0.997	0.635	0.003	0.197	0.985
1.020	3.447	0.997	0.948	0.717	0.040	0.179	0.709
1.990	0.957	1.000	0.999	0.785	0.000	0.005	0.929
2.000	1.438	0.999	0.997	0.642	0.003	0.114	0.974
2.005	0.417	1.000	0.999	0.853	0.001	0.024	0.969

TABLE VI. Long-time average probabilities (cf. text for details) as a function of laser frequency compared with the dipole function μ_3; $E_0=0.1$ for $\hbar\omega\approx 1.0$, $E_0=0.5$ for $\hbar\omega\approx 2.0$.

$\hbar\omega$	$\langle n\rangle$	P_b	P_{I}	P_{II}	P_N	P_c	P_c^{I}/P_c
0.995	5.599	0.915	0.932	0.481	0.063	0.229	0.733
1.000	4.739	0.997	0.962	0.546	0.032	0.242	0.846
1.005	4.121	0.999	0.995	0.600	0.005	0.188	0.974
1.985	1.623	0.999	0.998	0.736	0.001	0.139	0.990
1.990	1.843	0.999	0.998	0.682	0.002	0.184	0.988
2.020	2.123	0.999	0.966	0.563	0.033	0.352	0.904

sharpness of these peaks due to power broadening as E_0 increases. Similar sharp features appear in the overtone spectrum for μ_1, Fig. 2(b), particularly in the range $\hbar\omega=1.98$–2.03. The spectra for the dipole functions μ_2, μ_3, and μ_4 are shown in Figs. 3, 4, and 5, respectively. These spectra are generally similar to the spectrum of the μ_1 dipole function except that the multiphoton absorption peaks occur at somewhat different frequencies. In all four dipole functions $\langle n\rangle$ reaches peak values of between 5 and 6 near $\hbar\omega=1.0$ and of about 2 near $\hbar\omega=2.0$. Note that the multiphoton absorption is red-shifted from the single-photon fundamental or overtone frequencies. Further analysis of the spectra, particularly near $\hbar\omega=1.0$ and 2.0, is presented below in order to determine the extent of Q^{I} selectivity in this model system.

C. Long-time averaged probabilities

To demonstrate the extent of PSE in this system the following long-time averaged probabilities were evaluated: P_b, the probability of occupying a bound state below the classical dissociation barrier; P_{I}, P_{II}, and P_N, the probabilities of occupying a bound Q^{I}, Q^{II}, and N state, respectively; P_c and P_c^{I}, the probabilities of occupying a bound state and a bound Q^{I} state above the classical critical energy. These probabilities are obtained by summing the appropriate long-time transition probabilities, Eq. (2.14).

Results for the four dipole functions $\mu_1,\ldots,\mu_4$, are compiled in Tables IV–VII. The calculations were usually done near $\hbar\omega\approx 1.0$ and 2.0, i.e., the fundamental and overtone frequencies of the Q^{I} ladder. A more detailed analysis was performed for the dipole function μ_1 including a study of frequency and intensity dependences, and distribution of state probabilities.

The breakdown of spectral probabilities near the Q^{I} fundamental and overtone frequencies shows similar features for all four dipole functions. It is clear that near these frequencies the Q^{I} states are dominantly populated in the excitation process, Q^{II} states are highly populated whereas the probability of occupying N-type states is small and significantly increases only at large field intensities (cf. Table IV). This result is, however, somewhat misleading because the maximum average excitation always peaks around two $\hbar\omega=1.0$ photons below the critical energy, while the density of N states is substantial only above E_c. Obviously, the entire N-state probability is concentrated above the critical energy which is therefore the appropriate energy region to be considered with regard to PSE in this system. The probability of occupying Q^{II} states above E_c is negligible indicating that these states hardly participate in the multiphoton excitation at high energies. The high values of P_{II} are simply due to the fact that many low-lying states are simultaneously designated as Q^{I} and Q^{II} (cf. Table I in Ref. 19). The population probability above E_c is divided between Q^{I} and N-type states with the significant portion usually attributed to Q^{I} states. Comparing the columns for P_c and P_c^{I}/P_c (the fraction of P_c which is Q^{I}) in Tables IV–VII reveals several features in support of PSE via the Q^{I} ladder. First notice that within 1% of the Q^{I} fundamental and overtone frequencies P_c is always large (20–30%) with P_c^{I}/P_c the bigger fraction. For every dipole function there exists at least one "Q^{I} frequency" for which P_c is large and P_c^{I}/P_c is over 95%. The detailed frequency analysis in Table IV shows that as long as the frequency is near the Q^{I} fundamental or overtone, then efficient excitation above the critical energy occurs whether the laser is tuned on a peak or a valley in the corresponding multiphoton absorption spectra, Fig. 2. However, when the laser is largely off the Q^{I} frequencies, P_c^{I}/P_c reduces significantly indicating that mainly N states are now being populated above E_c. Similar effects are observed when the field intensity increases,

TABLE VII. Long-time average probabilities (cf. text for details) as a function of laser frequency computed with the dipole function μ_4; $E_0=0.1$ for $\hbar\omega\approx 1.0$, $E_0=0.5$ for $\hbar\omega\approx 2.0$.

$\hbar\omega$	$\langle n\rangle$	P_b	P_{I}	P_{II}	P_N	P_c	P_c^{I}/P_c
0.995	4.239	0.999	0.947	0.589	0.041	0.221	0.765
1.005	4.115	0.998	0.992	0.636	0.008	0.214	0.962
1.015	2.733	0.982	0.983	0.786	0.005	0.128	0.865
1.980	1.089	0.999	0.997	0.790	0.002	0.017	0.867
1.995	2.051	0.999	0.984	0.628	0.015	0.272	0.943
2.005	1.328	0.999	0.981	0.792	0.019	0.146	0.871

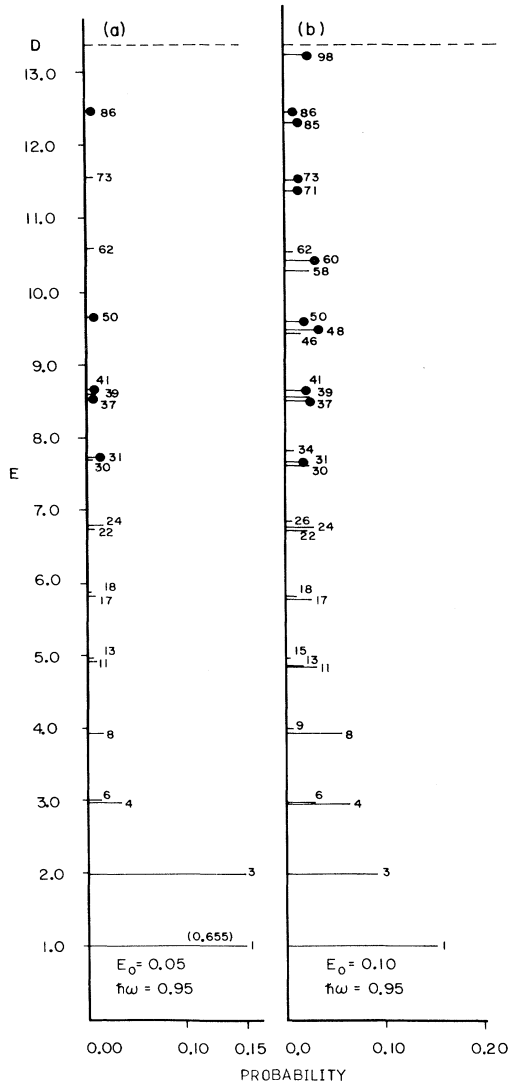

FIG. 6. Stick diagram showing long-time average transition probabilities from the ground state for the dipole function μ_1, computed at a frequency which is off the Q^1 fundamental. N states are indicated by a dot at the end of the stick. (a) $E_0=0.05$; (b) $E_0=0.1$.

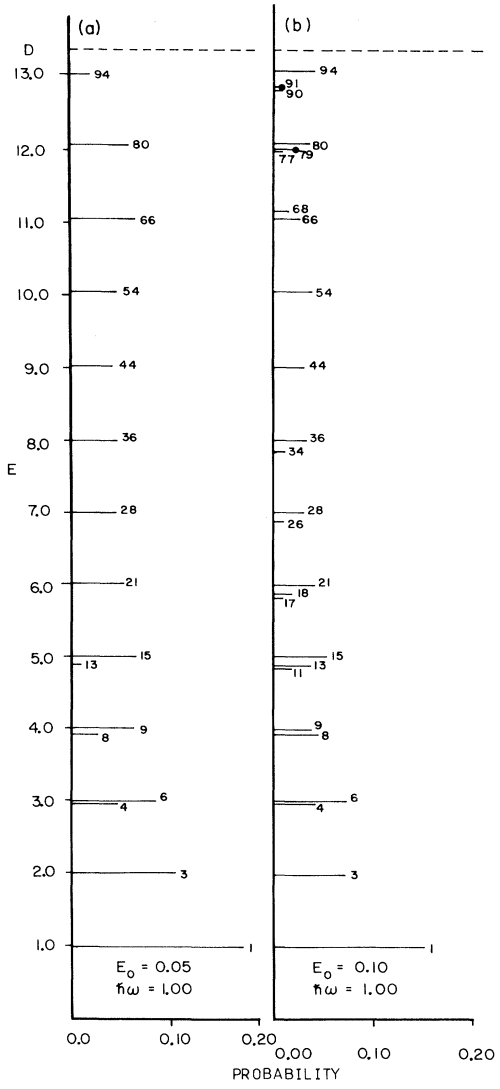

FIG. 7. Same as Fig. 6 but at Q^1 fundamental frequency.

on or off the preferred Q^1 frequencies. Note in particular that, when the frequency is largely detuned from the Q^1 ladder, then significant excitation above the critical energy is possible only at high field intensities. But at $\hbar\omega=1.0$, near the Q^1 fundamental, efficient excitation above E_c is achieved at the lowest field intensity $E_0=0.05$ (cf. Table IV).

Additional support to the Q^1 selective excitation route is found from examination of the dissociation probabilities given by $1-P_b$. Note that whenever P_c^1/P_c is large ($>95\%$), P_b is always about 99%, corresponding to a rather low dissociation probability. On the other hand, note that when P_c^1/P_c is low, i.e., when the N-state probability is large, P_b decreases to about 95%, which corresponds to a reasonable dissociation probability in such model system.[29,30] The reason for this surprising result is simply that the 110-state basis set used in the Floquet method calculations just misses the first Q^1 rung above the dissociation barrier (cf. states 111 and 112 in Table II). This state has about 40% weight on the TDHO states $(13,\pm13)$, it is therefore not a real quasiperiodic state according to the Hose-Taylor criterion. Nevertheless, this is exactly the continuum resonance that will carry most of the oscillator strength from the last Q^1 bound state. Realizing this fact we have performed a Floquet time-evolution calculation with 120 states including the "missed" Q^1 rung in the continuum. The resulting dissociation probabilities increased to reasonable values 3—5 %, without any significant change in P_c^1/P_c. Examination of the state transition probabilities showed that it is exactly the state 111 that accumulates probability above the dissociation barrier when $\hbar\omega=1.0$.

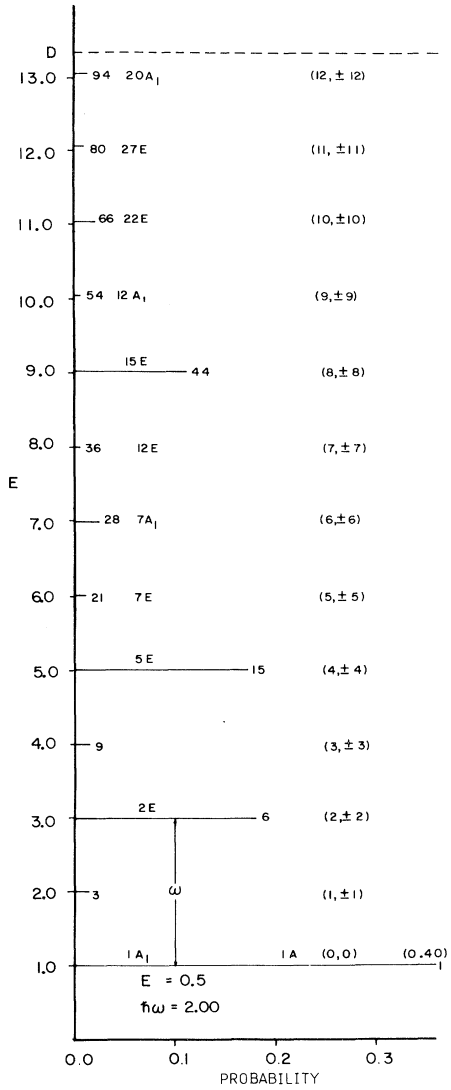

FIG. 8. Same as Fig. 6 but at Q^{I} overtone frequency.

A detailed analysis of the long-time averaged transition probabilities from the ground state to the jth state P_j is given for the dipole function μ_1. Figures 6–8 show stick diagrams of the transition probabilities at the corresponding energy levels. The states are labeled according to Tables I–III in Ref. 19; N states are indicated by dots at the end of the stick. Figures 6 and 7 display results obtained at $\hbar\omega=0.95$ and 1.0, respectively, at each of the two field strengths $E_0=0.05$ and 0.10. It is clear from Figs. 6 and 7 that there is a much greater tendency to occupy N states at the off-fundamental frequency $\hbar\omega=0.95$ than at the Q^{I} fundamental $\hbar\omega=1.0$. The population of N states increases as E_0 increases; this effect is much more pronounced off the Q^{I} fundamental. At $\hbar\omega=1.0$ and $E_0=0.10$ only two N states, 79 and 91, receive significant probability (>0.005). Note that Q^{I} ladder states are almost exclusively populated at $\hbar\omega=1.0$ and $E_0=0.05$, and are populated in the majority at $E_0=0.10$. The stick diagram at the overtone frequency $\hbar\omega=2.00$, Fig. 8, shows qualitatively similar features to Fig. 7; the Q^{I} ladder states with even n receiving virtually all of the probability.

At this stage we would like to point out that if the basis set on which the Floquet time-evolution calculations were performed had been much larger, we would not expect to see exactly the same long-time averaged transition probabilities. However, it does not seem reasonable to us that the inclusion of a true continuum above the classical dissociation barrier would significantly alter the main results drawn so far that at laser conditions appropriate for excitation of the Q^{I} ladder, PSE does occur in this system.

D. Time evolution of excitation probabilities

To complete the picture of selective excitation in this system, the time evolution of ground-state to excited-state transition probabilities, Eq. (2.12), is presented below. Figures 9–11 display stick diagrams of instantaneous transition probabilities at three times, $t=8\tau$, 16τ, and 24τ, computed for three different frequencies. In Fig. 9 the frequency is not favorable for multiphoton excitation above E_c. In fact, there is almost no excitation above state 11. At later times the probabilities merely Rabi-cycle

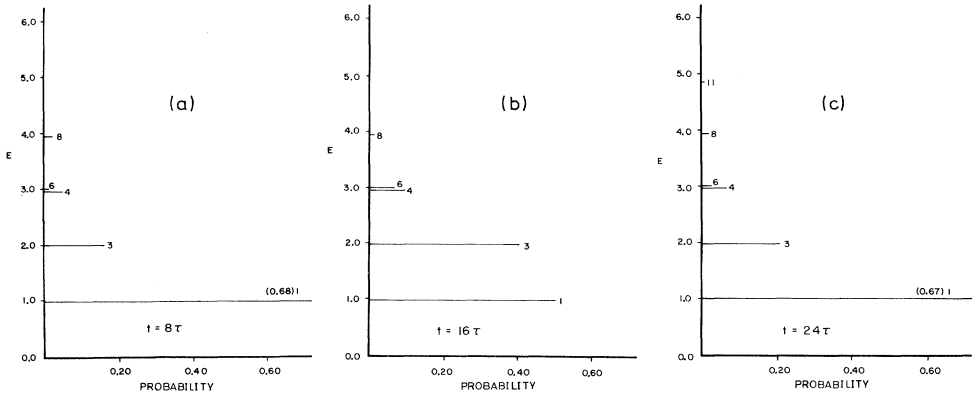

FIG. 9. Stick diagram showing the time evolution of transition probabilities from the ground state for the dipole function μ_1. $\hbar\omega=0.900$, $E_0=0.10$, and τ is the optical cycle, $\tau=2\pi/\omega$. N states are indicated by a dot at the end of the stick. (a) $t=8\tau$; (b) $t=16\tau$; (c) $t=24\tau$.

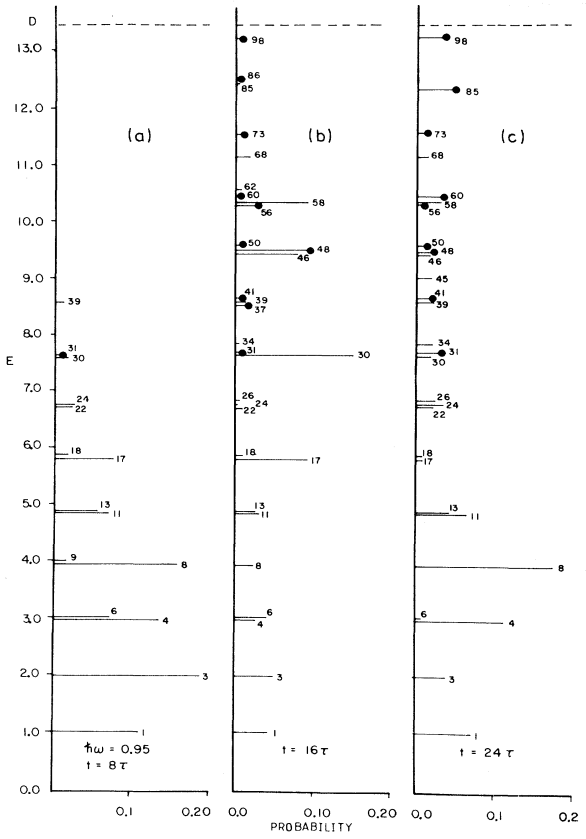

FIG. 10. Same as Fig. 9 but for $\hbar\omega = 0.95$ and $E_0 = 0.10$.

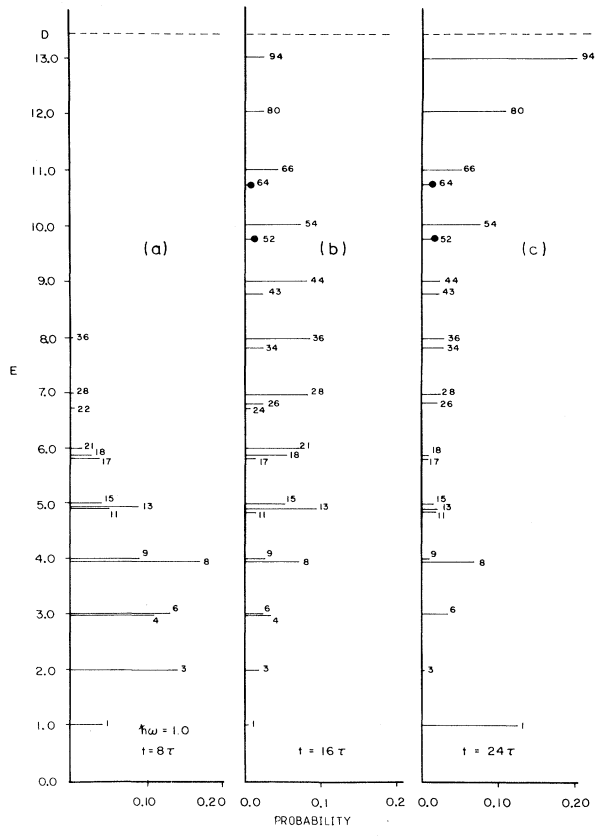

FIG. 11. Same as Fig. 9 but for $\hbar\omega = 1.00$ and $E_0 = 0.10$.

among six participating states. However, extensive excitation above the critical energy occurs when $\hbar\omega = 0.95$ (Fig. 10). At $t = 8\tau$, the only N state which is excited is state number 31. When $t = 16\tau$, several N states become occupied; states 46, 48, and 58 (all below E_c) have probabilities in excess of 0.05. Finally, when $t = 24\tau$, a number of high-energy states have probabilities in the range from 0.02 to 0.05. About ten N states above E_c are populated with probabilities greater than 0.01. Figure 11 shows the Q^{I} fundamental case, $\hbar\omega = 1.0$. There is clearly a large probability of occupying Q^{I} states above the critical energy. Only two N states, 52 and 64, are populated. Also note the large buildup in state 94 when $t = 24\tau$. However, for $t \geq 24\tau$, figures of this type do not accurately represent the dissociation dynamics; probability bumps appear at the top of the basis set due to its incompleteness.

IV. DISCUSSION

A. Summary: Mode-selective excitation in the Hénon-Heiles system

We have studied the quantum dynamics of laser-driven wave packets on the Hénon-Heiles potential surface. Floquet theory was used to generate the time propagator for the molecular eigenstates interacting with the classical laser field. Interest in the Hénon-Heiles potential was stimulated by classical dynamics studies showing that this system exhibits a regular (quasiperiodic) motion at low energies, whereas at high energies, above a critical energy, the classical motion is predominantly chaotic and typical of high mode-mode mixing with a low probability of finding non-mode-mixed quasiperiodic trajectories. Semiclassical[23] and quantal[19] studies on this system had shown that certain quantum levels correspond to quasiperiodic trajectories. These states, amenable to semiclassical quantization, were analyzed to be of two types: Q^{I}, the normal (harmonic) mode; and Q^{II}, a local (bond) mode.[19] Other states which are neither Q^{I} nor Q^{II} are denoted as N states, these are highly mode-mixed.

The quantum dynamics calculations show that efficient mode-selective multiphoton excitation up a ladder comprising Q^{I} states may be obtained by adjusting ω and E_0. The quantal wave packets representing the molecule in the laser field then contain almost exclusively Q^{I} states. Analysis of long-time averages revealed that with suitable laser conditions the probability of finding the system in a bound state above the critical energy was almost entirely in a Q^{I} state ($>95\%$). Note that in the graphs of $\langle n \rangle$, which are roughly the multiphoton absorption spectra, the system absorbs over an energy range that is 10% and is red-shifted from the fundamental or overtone frequencies. Table IV shows that even though absorption begins at

about $\hbar\omega=0.92$, at low field strengths very few states are populated above E_c until we reach $\hbar\omega=0.95$. As we get closer to the Q^{I} fundamental, lower powers are required to excite above the critical energy. Moreover, as the laser frequency approaches the Q^{I} fundamental or overtone, PSE via the Q^{I} ladder is much more pronounced. Selective excitation was more favorable for low E_0; increasing the field strength had a tendency to reduce the Q^{I} selectivity. Far from the Q^{I} fundamental, if the field intensity is large, significant population above E_c is obtained without occupying Q^{I} states by climbing a quasicontinuum of N states (cf. results for $\hbar\omega=0.90$ in Table IV). However, close to the Q^{I} fundamental significant population (of mainly Q^{I} states) above the critical energy is obtained with the use of much less power by climbing a mode-selective Q^{I} ladder. All these conclusions do not depend on the dipole function chosen to represent the coupling to the radiation field. It has been suggested[34] that chaotic time evolution does not necessarily defy selectivity. In Sec. IV C we shall explain the reasons why PSE does occur in this system, particularly at high energies in the classical chaotic region.

Waite and Miller[35] have recently considered a different aspect of mode selectivity in the Hénon-Heiles system, although with different potential parameters than the ones used here. They employed the complex coordinate method to compute the unimolecular decay rate of tunneling through the barriers for different quasibound eigenstates. The decay-rate constants they obtained showed that symmetry-induced mode specificity exists, but the rate constants for states of the same symmetry species (e.g., A_1, A_2, or E) increased with energy as predicted by standard statistical models and no apparent change was observed near the classical critical energy. However, even for the smallest value of $\hbar$ (0.02) considered in the Waite-Miller study the system had only about 35 quasibound states. A Hose-Taylor-type analysis showed that in this case there are very few N states, appearing only near the dissociation barrier. It is not suprising, therefore, that the Waite-Miller results did not show any apparent change moving from the classical quasiperiodic to the classical chaotic region. We intend to repeat the Waite-Miller calculation but for the potential parameters used in this study. This potential encompasses more quasibound states of the N type, particularly near E_c, and it would be interesting to see whether there are differences in the decay rate between states of type Q^{I}, Q^{II}, and N, which belong to the same symmetry species.

B. Mode-selective excitation in another anharmonic system

Using Floquet theory and the molecular Hamiltonian

$$H=-\tfrac{1}{2}\left[\frac{\partial^2}{\partial x^2}+\frac{\partial^2}{\partial y^2}\right]+\tfrac{1}{2}\omega_y y^2 +D(1-e^{-\alpha(x-\alpha y)})^2 \tag{4.1}$$

Davis and Wyatt[30] have recently studied the quantum dynamics of laser-driven wave packets. This system had been studied classically by Hänsel[31] and by Martin and Wyatt.[36] For the parameters listed in Ref. 36, the potential supports 117 bound states. The normal-mode frequencies are $\omega_x=919$ cm^{-1} and $\omega_y=1845$ cm^{-1}; this is a 1:2 Fermi resonant system. The potential well near the origin leads into a single dissociation valley along the X direction.

For the laser intensity $I=13$ GW/cm^2, plots of $\langle n\rangle$ versus $\hbar\omega$ were obtained through expansion of the time-dependent wave function in 150 eigenstates. These plots show a broad bimodal absorption profile extending from 650 to 1000 cm^{-1}, and a sharp "overtone" band between 1800 and 2000 cm^{-1}. At several frequencies, long-time averaged and instantaneous probabilities were calculated. There are again indications of mode-selective excitation. For example, when $\hbar\omega=1866$ cm^{-1}, at the center of the overtone peak, the quantal wave packet spreads dominantly on the molecular eigenstates having 0,1,2,3,... nodes along the Y axis as though this mode was being selectively excited. These results persisted up to 0.73 ps where about 90% of the probability lies between E_c and D. Note that the overtone frequency is approximately the frequency of the normal (uncoupled) Y mode. We intend to carry out Hose-Taylor-type analysis on this system to see whether there exists a Q^{I}-type ladder.

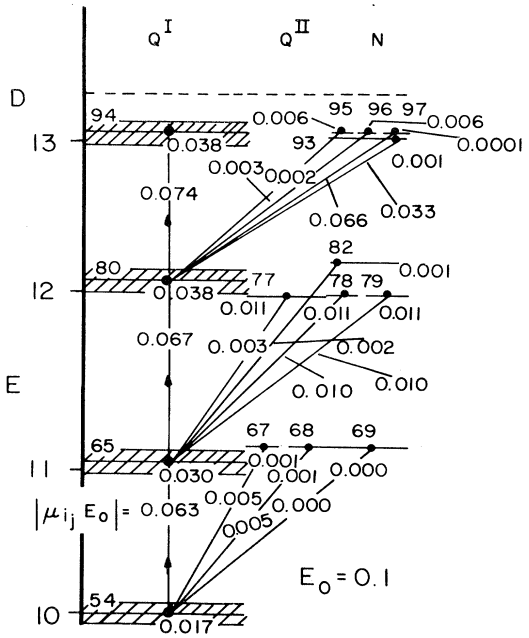

FIG. 12. μ_4 dipole couplings between Q^{I} ladder states to states separated by about $\hbar\omega=1.0$ in the top four bands below the classical dissociation barrier. Right column shows Q^{I} ladder states which are coupled by the laser field; the cross-hatched region near each Q^{I} rung indicates the power-broadening width $\pm|\mu_{j,j-1}E_0|$; the middle and right columns show Q^{II} and N states, respectively. Numbers below the states are long-time average transition probabilities; numbers on the lines connecting states to the Q^{I} rungs are coupling elements $|\mu_{i,j}E_0|$. Not all states in this energy range $10<\epsilon<D$ are shown.

C. Criteria for mode-selective excitation

The results of Sec. III clearly demonstrate that the Q^{I} ladder is an efficient route for selective multiphoton excitation in this model system. What is particularly interesting is the fact that at a particular laser frequency the probability of occupying a bound state in the chaotic region, above E_c, is relegated exclusively to a Q^{I} state. Note that in the chaotic region the Q^{I} states are in the minority. To explain these high probabilites of occupying Q^{I} states we consider a detailed analysis of the radiative couplings below.

Figure 12 shows the μ_4 dipole couplings between four bands of states near the classical dissociation limit, which are separated by about $\hbar\omega = 1.0$. The right column shows the Q^{I} ladder states which are coupled successively by the laser field. The cross-hatched region around each Q^{I} ladder state indicates the power broadening for single-photon transitions. The upper and lower edges of the jth band are given by $\epsilon_j \pm |\mu_{j,j-1}E_0|$, where $\mu_{j,j-1}$ is the matrix element of the μ_4 dipole function linking the successive Q^{I} ladder states j and $j-1$. The requirement for effective excitation up the Q^{I} ladder is

$$\epsilon_j - |\mu_{j,j-1}E_0| \leq \hbar\omega + \epsilon_{j-1} \leq \epsilon_j + |\mu_{j,j-1}E_0| \ . \tag{4.2}$$

This condition is always fulfilled in the Q^{I} ladder. The power broadening for the last four rungs at $E_0 = 0.1$ is about 12% as compared to detuning of less than 1% (cf. Table II). Note that $|\mu_{j,j-1}E_0|$ has about the same value between successive Q^{I} ladder states.

There are some Q^{II} and many N states which lie approximately within the power-broadened width of the Q^{I} ladder states; these Q^{II} and N states are shown on the middle-right and right columns of Fig. 12, respectively. A survey of the dipole matrix elements linking Q^{II} and N states from one band to the Q^{I} ladder states of an adjacent band has revealed that the $Q^{\mathrm{I}} \cdots N$ and $Q^{\mathrm{I}} \cdots Q^{\mathrm{II}}$ coupling elements are about an order of magnitude smaller than the $Q^{\mathrm{I}} \cdots Q^{\mathrm{I}}$ couplings. This is precisely the reason why excitation up the Q^{I} ladder is much more favorable. The fact that $Q^{\mathrm{I}} \cdots Q^{\mathrm{II}}$ and $Q^{\mathrm{I}} \cdots N$ dipole couplings are relatively small compared to the $Q^{\mathrm{I}} \cdots Q^{\mathrm{I}}$ couplings is predictable from the Hose-Taylor criterion defining Q^{I}, Q^{II}, and N states. This is because Q^{I} ladder states describe high excitation along one normal mode in the sense that the major part of the wave function is simply the normal-mode state itself. They cannot, therefore, efficiently couple radiatively to states which spread the excitation among many other modes. It is reasonable to expect that efficient radiative couplings occur between states of similar character (e.g., Q^{I} states). Note that this pseudo selection rule is analogous to the restricted quantum exchange model discussed by Thiele *et al.*[37] The radiative couplings between the Q^{I} ladder states must follow to a good approximation the selection rules of the separable system which was used to define the Q^{I}-type states (the TDHO in this case). If the sequence of Q^{I} states in the system follows favorable selection rules, then efficient PSE is possible, as is the case in this model system. It should be realized that the existence of Q^{I} states does not necessarily guarantee PSE. Other systems may exist in which sequences of Q^{I}-type states defy the favorable selection rules, in which case PSE will not occur.

Finally let us turn to a discussion of the effect of the field strength. As E_0 increases it is obvious that the radiative couplings will mix the Q^{I}, Q^{II}, and N states more strongly. The power-broadening width of the Q^{I} states will become larger and more N states will effectively couple to the Q^{I} ladder states. The net result would be a decrease in the probability of occupying Q^{I} states above E_c. This is exactly what is seen in the calculations shown in Table IV. We would also like to point out that at extremely high field intensities the Hose-Taylor analysis must be carried in the presence of the field. The reason is that the radiative couplings may exceed the potential anharmonicities in which case the "free-field" designation of states as Q^{I}, Q^{II}, and N is meaningless. In summary, to achieve PSE it is desirable to use mild field intensities but sufficient to compensate for detunings within the Q^{I} ladder.

D. Mode-selective excitation in real molecules

It is reasonable to assume that some molecules should have ladders of Q^{I}-type states extending above E_c into the quasicontinuum and continuum. Provided the dipole matrix elements connecting consecutive ladder states satisfy the pseudo selection rules, it should be possible to find laser conditions as to achieve mode-selective excitation in real molecules. The main difference between this model system and real molecules is the fact that real molecules certainly have a much higher density of states, and, in particular, of N-type states. As seen in the previous subsection, N states within the power-broadening range of a Q^{I} rung will "rob" oscillator strength from the selective ladder transition. On the other hand, it is also almost certain that $Q^{\mathrm{I}} \cdots N$ dipole couplings are much smaller than the $Q^{\mathrm{I}} \cdots Q^{\mathrm{I}}$ type. It remains to be seen which of these competing effects dominates in real molecules. Would the weak $Q^{\mathrm{I}} \cdots N$ couplings combined with the exceedingly high density of N states reduce the possibility of PSE, or, in turn, would pseudo selection rules, favoring selectivity, prevail?

There is some strong, but as yet admittedly incomplete, evidence that analogs of the Q^{I} ladder exist in real molecules. The strongest evidence is the experiment of Coggiola *et al.*[38] who create highly vibrationally excited CF_3X^+ ions, X=I, Br, and Cl, by electron impact ionization, and then show that they are able to dissociate the ion into $CF_3^+ + X$ using a *single ir photon* whose frequency distribution is *peaked* around one of the *ion fundamentals* with a width of about 30 cm^{-1}. The ions fundamentals are known from the spectroscopy of the Rydberg states of the corresponding neutrals whose surfaces are parallel those of the ions. They fail to dissociate the ion in the X=Cl case where the required ion fundamental is out of the frequency range of the laser. It is extremely hard to imagine that a quasicontinuum-to-continuum transition would require a near-fundamental frequency. Our model of a ladder that has rungs in both the quasicontinuum and the continuum exactly, but perhaps not uniquely, explains this experiment. It is necessary to realize that the excitation and dissociation processes must be thought of separately. Even if mode-mode mixing is not important in the excitation up the ladder rungs in the continuum, it could well be important in their decay. Hence, we say nothing about the dis-

sociation products. If decay widths consistent with the Rice-Ramsberger-Kassel-Marcus (RRKM) theory are assumed for Q^1-type rungs in the continuum, and give agreement with the experimental evidence, this would only persuade one that mode-mode mixing is important at this point. Interestingly, in the above experiment the $CF_3^+ + X$ has the lowest energy and is the statistically expected dissociation channel. Yet the excitation process seems to be definitely selective.

At this point we would like to note that even the ir mutliphoton dissociation of SF_6 to SF_5 and F, a reaction intimately related to the quasicontinuum model,[39] shows strong signs of being interpretable in terms of a ladder of Q^1-type states. In Fig. 6 of Bloembergen and Yablanovich[39] it is noted that at 1000 K, where SF_6 must on the average be in the quasicontinuum, the most favored absorption frequency peaks around the ν_3 fundamental with a width of about 40 cm^{-1}. The explanation given for this "surprising" result is that it is due to nonuniform distribution of oscillator strength.[39] Why would such nonuniform distributions exist in the quasicontinuum which is believed to be extensively mode-mode mixed? Perhaps much of the valuable work done on SF_6 should be reevaluated with the idea that Q^1-type ladders exist, as they perfectly explain such nonuniform distributions of oscillator strengths.[40]

ACKNOWLEDGMENTS

One of us (R.W.) was a vistor at the Institute for Molecular Science. He thanks members of the division of Theoretical Studies, particularly Hiroki Nakamura, Kauzo Takatsuka, and Keiji Morokuma, for their hospitality and research assistance. This work was supported by The National Science Foundation, Grants CHE-82-07152 and CHE-81-09576, and by a grant from the Robert A. Welch Foundation.

*Permanent address: Department of Chemistry, University of Texas, Austin, Texas 78712.

†Permanent address: Department of Chemistry, University of Southern California, University Park, Los Angeles, California 90089-0482.

[1]A. H. Zewail, Phys. Today 33, No. 11, 27 (1980).

[2]V. S. Letokhov, Phys. Today 33, No. 11, 34 (1980).

[3]Y. T. Lee and Y. R. Shen, Phys. Today 33, No. 11, 52 (1980).

[4]J. Jortner and R. D. Levine, Adv. Chem. Phys. 47, 1 (1981).

[5]A. Ben-shaul, Y. Haas, K. L. Kompa, and R. D. Levine, *Laser and Chemical Change* (Springer, New York, 1981), pp. 421—423 and 454—458.

[6]D. S. King, *Dynamics of the Excited State,* edited by K. P. Lawley (Wiley, New York, 1982), p. 105.

[7]R. Naaman, D. M. Lubman, and R. N. Zare, J. Chem. Phys. 71, 4192 (1979).

[8]R. B. Hall and A. Kaldor, J. Chem. Phys. 70, 4027 (1979).

[9]R. E. Smalley, D. H. Levy, and L. Wharton, J. Chem. Phys. 64, 3266 (1976); M. S. Kim, R. E. Smalley, L. Wharton, and D. H. Levy, *ibid.* 65, 1216 (1976).

[10]K. V. Reddy and M. J. Berry, Chem. Phys. Lett. 66, 223 (1979).

[11]D. W. Noid, C. Bottcher, and M. L. Koszykowski, Chem. Phys. Lett. 72, 397 (1980).

[12]I. C. Percival, J. Phys. B 6, L229 (1973).

[13]J. Ford, Adv. Chem. Phys. 24, 155 (1973).

[14]M. V. Berry, in *Topics in Nonlinear Mechanics (La Jolla Institute),* Proceedings of the Workshop on Topics in Nonlinear Dynamics, AIP Conf. Proc. No. 46, edited by S. Jorna (AIP, New York, 1978), p. 16.

[15]S. A. Rice, in *Advances in Laser Chemistry,* edited by A. H. Zewail (Springer, New York, 1978), p. 2; Adv. Chem. Phys. 47, 115 (1981).

[16]R. A. Marcus, D. W. Noid, and M. L. Koszykowski, in *Advances in Laser Chemistry,* edited by A. H. Zewail (Springer, New York, 1978), p. 298; D. W. Noid, M. L. Koszykowski, and R. A. Marcus, Annu. Rev. Phys. Chem. 32, 267 (1981).

[17]M. Tabor, Adv. Chem. Phys. 46, 73 (1980).

[18]P. Brumer, Adv. Chem. Phys. 47, 201 (1981).

[19]G. Hose and H. S. Taylor, J. Chem. Phys. 76, 5356 (1982).

[20]I. C. Percival, Adv. Chem. Phys. 36, 1 (1977).

[21]R. A. Marcus, Discuss. Faraday Soc. 55, 34 (1973); W. Eastes and R. A. Marcus, J. Chem. Phys. 61, 4301 (1974).

[22]K. S. Sorbie and N. C. Handy, Mol. Phys. 32, 1327 (1976); K. S. Sorbie, *ibid.* 33, 1577 (1976).

[23]D. W. Noid and R. A. Marcus, J. Chem. Phys. 62, 2119 (1975); 67, 559 (1977).

[24]E. J. Heller and M. J. Davis, J. Chem. Phys. 75, 246 (1981).

[25]M. Hénon and C. Heiles, Astron. J. 69, 73 (1964).

[26]D. W. Noid and M. L. Koszykowski, Chem. Phys. 73, 114 (1980).

[27]R. J. Wolf and W. L. Hase, J. Chem. Phys. 73, 3379 (1980).

[28]L. D. Thomas and H. S. Taylor, Phys. Lett. 28, 1091 (1972).

[29](a) S. C. Leasure, K. F. Milfeld, and R. E. Wyatt, J. Chem. Phys. 74, 6197 (1981); (b) S. C. Leasure and R. E. Wyatt, Opt. Eng. 19, 46 (1980); (c) K. F. Milfeld and R. E. Wyatt, Phys. Rev. A 27, 72 (1983).

[30]M. J. Davis, R. E. Wyatt, and C. Leforestier, in *Intramolecular Dynamics: Proceedings of the 1982 Jerusalem Symposium,* edited by J. Jortner and B. Pullman (Reidel, Dordrecht, 1982); M. J. Davis and R. E. Wyatt (unpublished).

[31]K. D. Hänsel, Chem. Phys. Lett. 57, 619 (1978).

[32]G. Hose (unpublished).

[33]D. W. Noid, M. L. Koszykowsky, M. Tabor, and R. A. Marcus, J. Chem. Phys. 72, 6169 (1980).

[34]R. D. Levine, Chem. Phys. Lett. 76, 254 (1980).

[35]B. A. Waite and W. H. Miller, J. Chem. Phys. 74, 3910 (1981).

[36]D. L. Martin and R. E. Wyatt, Chem. Phys. 64, 203 (1982).

[37]E. Thiele, M. F. Goodman, and J. Stone, Chem. Phys. Lett. 69, 18 (1980).

[38]M. J. Coggiola, P. C. Cosby, and J. R. Peterson, J. Chem. Phys. 72, 6507 (1980).

[39]N. Bloembergen and E. Yablanovitch, Phys. Today 31, No. 5, 23 (1978).

[40]C. D. Cantrell, V. S. Letokhov, and A. A. Makarov, in *Coherent Nonlinear Optics: Recent Advances,* Vol. 21 of *Springer Topics in Current Physics,* edited by M. S. Feld and V. S. Letokhov (Springer, New York, 1981), Chap. 5.